SAND2019-1496C

Proceedings of the 2019 Hypervelocity Impact Symposium
HVIS2019
April 14-19, 2019, Destin, FL, USA
HVIS2019-031

Equation of State of Corning0120 High-Lead Glass Subject Shock Loading

Bernardo Farfan[a] William Reinhart[a] and Scott Alexander[a]

[a]*Sandia National Laboratories, Albuquerque, NM, 87185*

Abstract

Equation of state properties were studied for the high-lead glass Corning 0120, which is a potash-soda-lead glass also referred to as G12. This glass, which contains approximately 30% PbO by weight and has a density, ρ_o, of 3.034 g/cm^3 possesses properties suitable for many applications in industry such as optical components for space exploration instrumentation. Further understanding of its mechanical properties is desired for more complex applications in various fields, including applications where the glass may experience high-pressure shock loading. In this work plate impact experiments were conducted to determine the dynamic response of Corning 0120 at high stress levels. Tests were conducted over the pressure range from approximately 5 to 25 GPa utilizing the 90 mm bore single-stage powder driven gas gun at the Sandia National Laboratories STAR Facility. For this study, we used one-inch diameter Corning 0120 glass samples of two different thicknesses (3 mm and 7 mm) to use the evolution of the shock wave propagation through the material for analysis. The time-resolved material response was measured by means of a Velocity Interferometer System for Any Reflector system (VISAR). Results will be presented detailing the high-pressure shock loading response characteristics of the high-lead glass Coning 0120. Comparisons are made with similar results for lead free glass to assess the most prominent changes compared to lower density glasses and other lead filled glasses.

Keywords: High-lead glass, Equation of State, Hugoniot states.

Nomenclature

ρ	Density (g/m^3)
σ_x	Uniaxial stress (GPa)
σ_x^{HEL}	Hugoniot Elastic Limit (GPa)
U_s	Shock velocity (mm/us)
u_p	Particle velocity (mm/us)
C_L	Longitudinal speed of sound (mm/us)
C_o, S	Coefficients of linear relation $U_s = C_0 + S\ u_p$
ν	Poisson ration

1. Introduction

High-lead glass Corning 0120, also known in the industry as G12, is a material of interest for applications where the glass may experience extreme shock loading conditions such as optical components for space exploration instrumentation [1]. High-lead glasses exhibit lower Young's modulus and slow crack growth exponent as compared to lead free soda-lime silica glass or high purity glasses such as fused silica [1] [2] and it's an ideal candidate for mission critical applications. To adequately implement lead filled glasses for high stress applications designers need to understand the response of Corning 0120 glass under shock loading. Computational models are usually the tool of choice to aid the design process for a rapid turnaround of simulated shock conditions. However, numerical simulations rely on accurate experimental data to inform high fidelity material models to have the ability to precisely represent the material under shock conditions. The study presented in this work is intended to support future numerical models and general understanding of Corning 0120 glass with experimental data in a region of interest for the scientific community working in the field.

Sandia National Laboratories is a multimission laboratory managed and operated by National Technology & Engineering Solutions of Sandia, LLC, a wholly owned subsidiary of Honeywell International Inc., for the U.S. Department of Energy's National Nuclear Security Administration under contract DE-NA0003525.

Corning 0120 is a potash-soda-lead glass with the chemical composition $55SiO_2$-$3B_2O_3$-$4Na_2O$-$9K_2O$-$27PbO$-$2Al_2O_3$ and contains approximately 30% PbO by weight and has a density, ρ_o, of 3.034 g/cm^3 [3] [4]. Glasses modified with oxides such as PbO exhibit lower fracture toughness and are more susceptible to stress corrosion. Like many glasses, silicon dioxide, SiO2, forms the basis of Corning 0120. By employing the random network model [5] for amorphous solids, the glass structure can have ions that play the role of either network former or modifiers. Weaker ionic bonding leads to network modification while stronger orbital bonding leads to formation. The role of Pb as a modifier or former is still debated [6] but the different glass compositions and filler types can be associated to changes in the material response to shock loading. This paper considers the high-pressure shock loading response of Corning 0120 glass and comparisons are made with similar results for lead free glass [7] and other lead filled glasses [8] to assess its loading paths and mechanical deformation regions characteristics. Incremental and two-wave analysis were performed to study the elastic region and Hugoniot states respectively. We investigated the pressure range from approximately 5 to 25 GPa which covers most useful applications.

2. Experimental

Plate impact experiments were conducted utilizing the 90 mm bore powder driven gas gun at the Sandia National Laboratories Shock Thermodynamics Applied Research (STAR) Facility. The experimental configuration, shown in Fig. 1, is designed to measure the shock wave transmitted through the sample material at two different distances to study the shock response as well as the wave evolution through the material. The target plate includes two 1 inch in diameter Coning 0120 glass samples of different thicknesses each backed with a Lithium Fluoride (LiF) window coated by a thin layer of vapor deposited aluminum on the sample interface. The velocity of the sample–window interface is monitored with a VISAR [9]. Adjacent and flush to each sample we installed smaller LiF windows, vapor deposited in the same manner as described above, to monitor shock time of arrival (TOA) to calculate closing impact times. These TOA windows were monitored with the same VISAR system. The target plate is impacted with a phenolic projectile faced with a thick copper impactor traveling at a range of velocities. The thickness of the impactor is designed to avoid early rarefactions that could possibly disrupt the plane shock wave formation and propagation through the sample. The velocity and tilt of the impactor/target impact was recorded with a set of electric trigger pins.

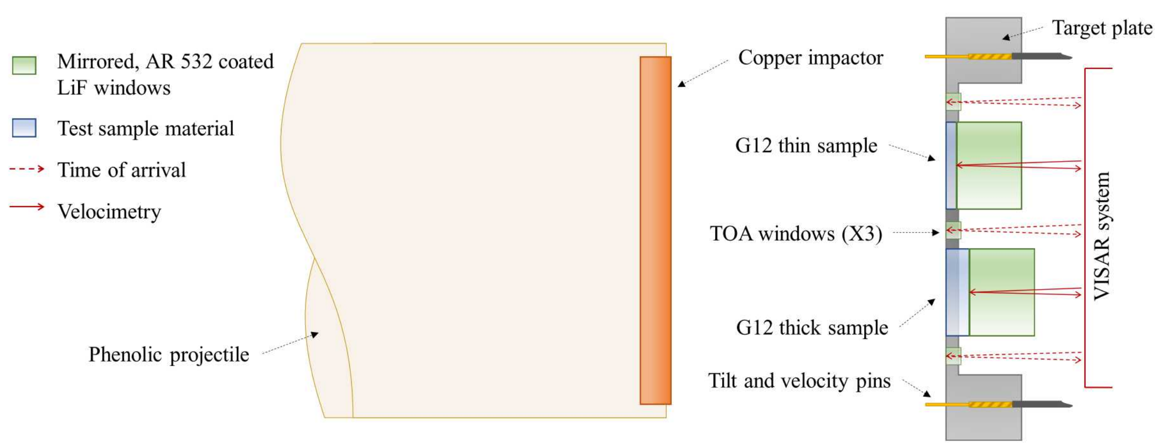

Fig. 1. Illustration of double sample plate impact experimental configuration for Corning 0120 glass at high velocity impact.

Table 1 shows the details of the experiments performed for this work. Four independent experiments were performed with two Corning 0120 samples from the same lot of approximately 3 mm and 7 mm thick for each shot. Ultrasonic measurement of the samples was used to determine the longitudinal elastic wave velocity (C_L) in the material at zero stress as well as Young modulus (Y) and Poisson ratios (v). The samples were impacted with a 12.7 mm copper projectile at a range of velocities from 0.52 km/s to 2.00 km/s, these impact velocities generated stress levels from 4.99 GPa to 25.00 GPa in the sample interface.

Table 1. Experimental details

Shot ID	Sample thickness (mm)		C_L (mm/us)	Y (GPa)	v	Impact Velocity (km/s)	Stress (GPa)
HORSE - 1	A: 7.015	B: 3.005	4.834	60.08	0.240	0.52	4.79
HORSE - 2	A: 7.015	B: 3.010	4.808	59.77	0.237	0.91	8.57
HORSE - 3	A: 7.023	B: 3.007	4.759	59.44	0.228	1.31	13.39
HORSE - 4	A: 7.018	B: 3.015	4.800	59.77	0.235	1.86	20.95
HORSE - 5	A: 7.025	B: 3.007	4.782	59.80	0.237	2.00	23.46

3. Results and discussions

3.1. Wave profiles

Wave profiles were obtained at two different propagation distances using the two sample thicknesses in the experimental setup described above. The data collected for the time-resolved velocity at the sample/window interface is plotted in Fig. 2, where the wave profile formation and propagation are observed, the thick sample data was shifted by one unit for visualization purposes. By looking at the wave profiles we can see that the two lowest pressure shots (HORSE 1 and 2) are mostly in the elastic region where deformation is reversible. Experiment HORSE-3 exhibits what it seems like the initial formation of a dispersed plastic shock somewhere after the Hugoniot Elastic Limit (HEL) where densification begins to occur resulting in irreversible deformation of the material. Subsequent experiments (HORSE 4 and 5) show a more definite and steeper formation of a plastic shock wave in the material at the higher stress levels. It has been reported in the literature that glass structures such as fused quartz and borosilicate glass exhibit a complex response, as seen in this data, when subjected to plane shock wave dynamic loading [7] [10]. Lower density glass response usually starts with an initial elastic ramp of the stress, or particle velocity, followed by a steep rise to the HEL. This, unusual behavior has been attributed to the decreasing elastic moduli of these glasses with pressure [11]. Highly modified glasses such as soda-lime lack the initial elastic ramp region due to densification [7] [8].

.

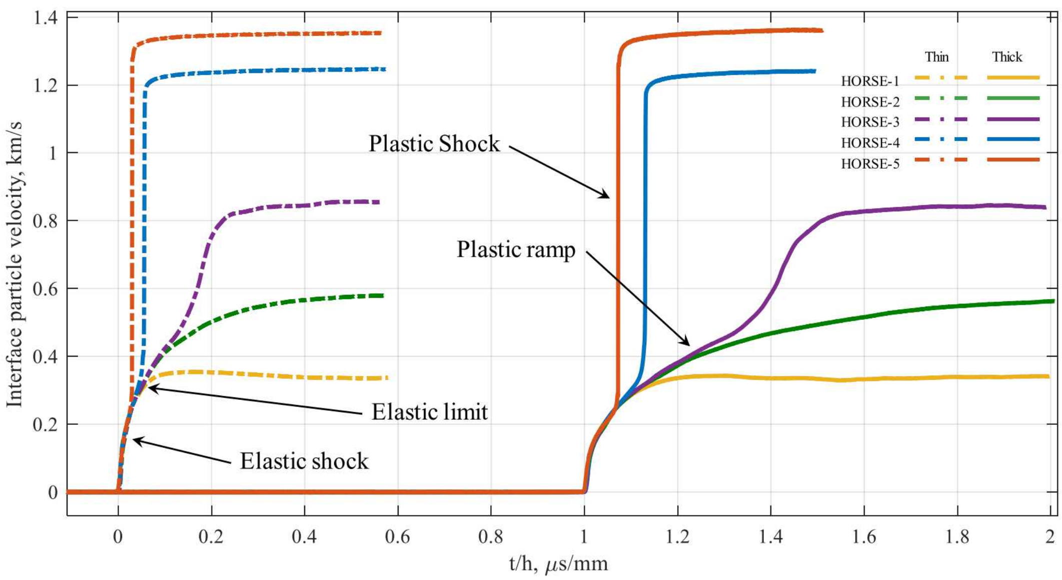

Fig. 2. Time resolved wave profiles of high-lead Corning 0120 glass at different propagation distances (thick sample data shifted by one unit).

By comparing the dynamic shock loading response of the potash-soda-lead Corning 0120 glass to low density glasses we can say that its response is like the one of soda-lime glass [7]. The wave profiles show, in order of arrival, an elastic shock, a plastic ramp, and a plastic shock as labeled in Fig 2. Higher density lead-filled glasses such as type D, extra dense flint glass (DEFE), ρ_o, of 5.18 g/cm^3 show an extremely fast rise response and a breakage in its slope [10] characteristic of ceramics not seen in the Corning 0120 glass studied here. It can also be observed that the experimental series have not overdriven the HEL level by the still evident elastic region at the highest stress level of 25.00 GPa in experiment HORSE-5. The experimental series has covered the transition from the elastic to the plastic region pressure range. The loading paths and mechanical deformation regions will be discussed in the following sections.

3.2. Hugoniot characterization

Hugoniot states were measured by conducting a series of experiments varying the impact velocity on the Corning 0120/LiF samples from 0.5-2 km/s which resolved the wave profiles shown in Fig 2. The foot of the elastic wave will travel at the wave velocity at zero-stress, thus, the time of arrival at the measurement interface relative to impact can be calculated from the thickness of the sample divided by the zero-stress elastic wave speed. This data is used as a fiducial to determine the time of impact. The zero-stress longitudinal wave velocities C_L were obtained by ultrasonic measurement of each sample before testing. By this absolute time reference, we can determine the wave speed of each component of the wave profile by Lagrangian analysis. The Rankine–Hugoniot equations describe the relationship between the shock wave speed, the particle velocity in the material, the stress and the density of the material. Impedance matching is used to determine the *in-situ* particle velocity from that measured at the sample/window interface and to uniquely define the Hugoniot state.

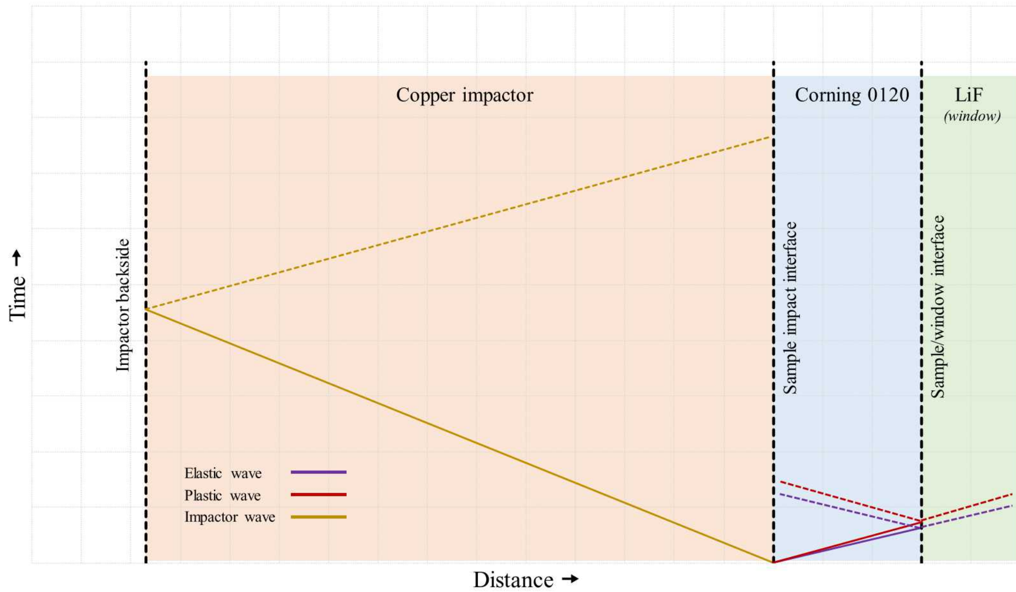

Fig. 3. X-t diagram of plate impact experiments on Corning 0120.

Fig 3. Shows a general X-t diagram of the plate impact experiments executed in this work. A shock is generated at the sample impact interface between impactor and sample producing an elastic and plastic wave traveling through the sample material (the experimental series did not overdrive the elastic wave). The traveling waves reach the window interface where the in-material particle velocities are measured. Incremental and two-wave analysis were performed to study the elastic region and Hugoniot states respectively. The Hugoniot elastic limit stress, (σ_x^{HEL}), is determined using the relation:

$$\sigma_x^{HEL} = \rho_o C_L u_e$$

where ρ_o is the initial density of the glass, and u_e is the in-material particle velocity measurement prior to transition to a plastic wave. The in-material particle velocity is determined through the impedance matching relation:

$$u_m = \frac{u_w(Z_w + Z_m)}{2Z_m}$$

where u_w, Z_w, and Z_m are the measured velocity in the window material, and the shock impedances of the lithium-fluoride window and the glass material, respectively. The loading path of the elastic region can be determined from transmitted wave experimental data. Utilizing the method of characteristics [12], an incremental analysis of the differential form of the Rankine–Hugoniot equations can be found from the time resolved velocity history data.

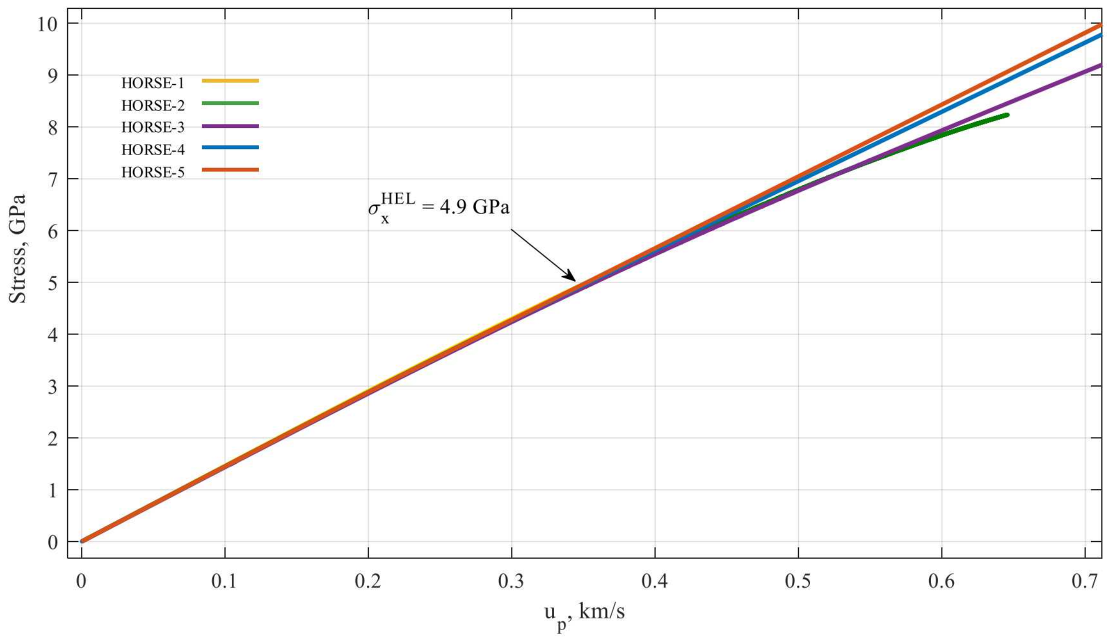

Fig. 4. Loading paths for Corning 0120 glass. Arrow indicate the point where divergence occurs representing stresses above the HEL level.

Applying the Rankine–Hugoniot equations by and incremental analysis, the pressure–particle velocity of the target can be found from the time resolved velocity history data obtained. Fig.4 shows the resulting loading paths for Corning 0120 glass from the data obtained in the experimental series. When a material is shocked at a stress level where the elastic deformation has not been overdriven, the material will exhibit an elastic response which is independent from the ultimate stress level the material is shocked to. Therefore, when elastic, the loading paths will be identical regardless of the final stress state. The point where the loading paths begin to deviate from each other is indicative of the HEL. The incremental analysis was applied through the plastic shock region to be able to distinguish the divergence where HEL occurs. By analyzing the loading paths in Fig 4 we can identify that the HEL for Corning 0120 is around 4.9 GPa.

The planar impact produces a compressive wave of uniaxial strain, which propagates across the target specimen and into the lithium-fluoride window. The measured velocity exhibits a two-wave structure. The subsequent structure following the elastic precursor represents pressure hardening of the material and this two-wave structure is the result of a transition from elastic to plastic deformation. As compression within the shock increases during the shock loading process, shear stresses will exceed the critical strength of the material (HEL) and plastic deformation occurs in the observed second wave. Because finite rise times are measured for the plastic wave, the plastic-wave velocity, U_{sp}, is taken at the center of the wave profiles of the different known thicknesses. For the Hugoniot states, or plastic region, a two-wave analysis was used by the following relation.

$$\sigma_{ph} = \sigma_e + \rho_e U_{sp}(u_{ph} - u_e)$$

Where σ_{ph} , u_{ph} are the plastic wave stress and particle velocity, and σ_e, u_e, ρ_e are the elastic wave stress, particle velocity and density behind the wave. Table 2 shows the Hugoniot parameters of the experimental series were a plastic shock wave formation has been observed overcoming the HEL of Corning 0120.

Table 2. Hugoniot summary

Shot ID	Impact Velocity (km/s)	U_{sp} (mm/us)	u_p (mm/us)	Strain	σ_{ph} (GPa)
HORSE - 1	0.52	-	-	-	-
HORSE - 2	0.91	-	-	-	-
HORSE - 3	1.31	3.6815	1.0374	0.246	13.39
HORSE - 4	1.86	4.4191	1.4509	0.320	20.95
HORSE - 5	2.00	4.5764	1.5802	0.319	23.46

3.3. Wave velocities

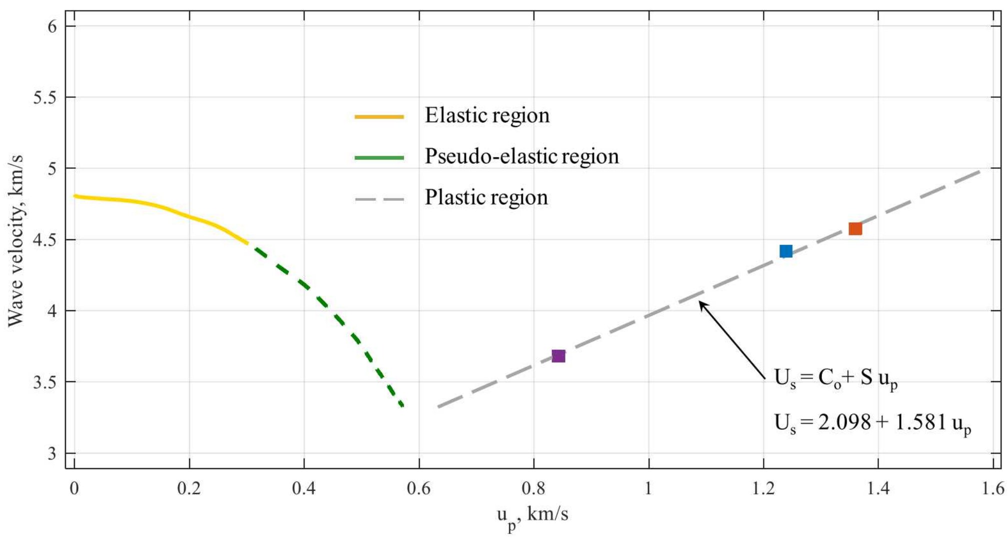

Fig. 5. Wave velocity/particle velocity relationship from experimental data illustrating the different regions of Corning 0120 glass under shock conditions. The initial elastic region at low pressures, the pseudo-elastic region, and the plastic fitted Us–up relation for the plastic region at higher pressures.

The wave velocity to particle velocity relationship can be used to describe the material response to dynamic shock loading. Fig 4 shows this relation for the Corning 0120 glass studied in this work. The solid yellow curve indicates the elastic region and is the differential analysis of the elastic portion of the wave profiles (HORSE 1-5) that overlap before they start diverging. The green dashed curve represents the pseudo-elastic region where plastic deformation has begun to occur, as evidenced by loading paths dependent on the final states, but no clear plastic shock wave is yet observed. Experiment HORSE-2 is a good representation of this state and defines the green dashed curve for the pseudo-elastic region. The rest of the experiments (HORSE 3-5), where a plastic shock wave is readily apparent, define the plastic region by the linear U_s-u_p relation represented by the gray dashed line.

The relationship in Fig 5 shows the initial negative dependence of wave velocity on particle velocity characteristic of glass materials. It is important to notice that after passing the HEL of 4.9 GPa (end of yellow line) determined in Fig 3, the loading path continues through the negative pseudo-elastic region (green dashed line), so the material responds pseudo-elastically up to 7.5 GPa before the formation of a plastic shock wave. Above this limit, the shock wave velocity is linear with respect to particle velocity and is well described by the general form of the relation $U_s=C_o+Su_p$ where C_o is the bulk wave speed and S is a dimensionless parameter describing the slope of the line.

4. Conclusions

High-lead glass Corning 0120 was studied under high-pressure dynamic shock loading to determine its response in the pressure range of 5 to 25 Gpa which is relevant to many applications. The shock loading response of this potash-soda-lead Corning 0120 glass is more similar to the lead-free soda-lime glass [7] than a higher density lead filled glasses such as DEDF [10]. The wave profiles show, in order of arrival, an elastic shock, a plastic ramp, and a plastic shock. The elastic region prolongs to its HEL and continues through a negative dependent pseudo-elastic response to higher pressures before entering the plastic region. The HEL determined for Corning 0120 is higher than soda-lime and DEDF. DEFE glass with a density of 5.18 g/cm^3 has a HEL of 4.3 GPa, and soda-lime with 2.49 g/cm^3 has a HEL of 4 GPa compared to Corning 0120 with a density of 3.03 g/cm^3 which has a HEL of 4.9 GPa. The linear U_s-u_p relation that represent experimental Hugoniot data is defined by the coefficients C_o =2.098, s=1.581.

Acknowledgements

This paper describes objective technical results and analysis. Any subjective views or opinions that might be expressed in the paper do not necessarily represent the views of the U.S. Department of Energy or the United States Government.

Sandia National Laboratories is a multimission laboratory managed and operated by National Technology & Engineering Solutions of Sandia, LLC, a wholly owned subsidiary of Honeywell International Inc., for the U.S. Department of Energy's National Nuclear Security Administration under contract DE-NA0003525.

References

[1] J. A. Salem, N. A. Smith and A. Ersahim, "Mechanical Properties of a High Lead Glass Used in the Mars Organic Molecule Analyzer," NASA STI Program, Cleveland, Ohio, 2015.
[2] J. A. Salem and R. Tandon, "Test Method Variability in Slow Crack Growth Properties of Sealing Glasses," NASA STI Program, Cleveland, Ohio, 2010.
[3] J. Sanghera and I. D. Aggarwal, Infrared Fiber Optics, Washington DC.: Naval Research Laboratories, 1998.
[4] C. A. Harper, Handbook of Ceramics, Glasses, and Diamonds, McGraw-Hill, 2001.
[5] W. D. Kingery, H. K. Bowen and D. R. Uhlmann, "Chapter 3," in Introduction to Ceramics, New York, John Wiley & Sons, 1972, pp. 91-124.
[6] I. B. Kacem, L. Gautron, D. Coillot and D. R. Neuville, "Structure and Properties of Lead Silicate Glasses and Melts," Chemical Geology, Elsevier, vol. 461, pp. 104-114, 2017.
[7] C. S. Alexander, L. C. Chhabildas, W. D. Reinhart and D. W. Templeton, "Changes to the shock response of fused quartz due to glass modification," International Journal of Impact Engineering, pp. 1376-1385, 2008.
[8] J. C. F. Millett and N. K. Bourne, "Direct measurements of strain in a shock-loaded, lead filled glass," Journal of Applied Physics, vol. 87, no. 8457, 2000.
[9] L. M. Barker, "Laser Interferometry in Shock-wave Research," Experimental Mechanics, vol. 12, 1972.
[10] N. K. Bourne, Z. Rosenberg and J. C. F. Millett, "The Plate Impact Response of Three Glasses," Transactions on the Built Environment, vol. 22, pp. 553-562, 1996.
[11] K. Kondo, S. Iio and A. Sawaoka, "Nonlinear pressure dependence of the elastic moduli of fused quartz up to 3 GPa," Journal of Applied Physics, vol. 52, no. 2826, 1981.
[12] D. E. Grady and E. G. Young, "Evaluation of Consitutive Properties From Velocity Interferometer Data," SAND 75-0650, Albuquerque, 1975.
[13] J. Wackerle, "Shock-wave Compression of Quartz," Journal of Applied Physiscs, vol. 33, no. 3, pp. 922-936, 1962.
[14] "Direct measurements of strain in a shock-loaded, lead filled glass," Journal of Applied Physics, vol. 12, no. 8457, pp. 8457-8460, 2000.